URSI GASS 2023, Sapporo, Japan, 19 – 26 August 2023

Chorus Wave Observations from Van Allen Probes: Quantifying the Impact of the Sheath Corrected Electric Field

David P. Hartley* [(1)], Ivar W. Christopher [(1)], Craig A. Kletzing [(1)], William S. Kurth [(1)],
Ondrej Santolik [(2, 3)], Ivana Kolmasova [(2, 3)], Matthew R. Argall [(4)], Narges Ahmadi [(5)]
(1) University of Iowa, Iowa City, IA, USA; e-mail: david-hartley@uiowa.edu; ivar-christopher@uiowa.edu; craig-kletzing@uiowa.edu; william-kurth@uiowa.edu
(2) Institute of Atmospheric Physics, Prague, Czech Republic; email: os@ufa.cas.cz; iko@ufa.cas.cz
(3) Charles University, Prague, Czech Republic; email: os@ufa.cas.cz; iko@ufa.cas.cz
(4) University of New Hampshire, Durham, NH, USA; email: matthew.argall@unh.edu
(5) University of Colorado, Boulder, CO, USA; email: narges.ahmadi@lasp.colorado.edu

Abstract

A technique has recently been established to quantify the variable coupling impedance between the electric field spherical double probes sensors on the Van Allen Probes and the magnetospheric plasma. A sheath impedance model has been developed to describe how this instrument-plasma coupling affects the amplitude and phase of electric field wave measurements. A full sheath-corrected EMFISIS dataset has been produced. Here, we quantify how measured chorus wave properties, including electric field wave power and the Poynting vector, are impacted by the sheath correction. This is achieved by performing a direct comparison between the uncorrected and sheath-corrected datasets. It is found that the sheath-corrected electric field chorus wave power is typically 2-9 times larger than the uncorrected measurement, depending on wave frequency. The sheath correction typically increases the Poynting flux by a factor of ~2, and causes the polar angle of the Poynting vector, θ_S, to switch hemisphere from parallel to anti-parallel propagation in ~2% of cases. The uncorrected data exhibit significant deviations from the theoretically predicted relationship between the wave vector and the Poynting vector, whereas this relationship is well-reproduced with the sheath-corrected data.

1 Introduction

The Van Allen Probes measured the wave electric field using spherical double probe sensors mounted on long centrifugally deployed wire booms in the spin-plane, with shorter rigid booms along the spin-axis. Intervals of favorable wave, magnetic field, and antenna geometry have been used to calculate each component of the whistler-mode wave electric field from magnetic field observations and cold plasma theory. A direct comparison between these theoretically predicted values, and those measured by the spacecraft, allowed for the variable coupling impedance between the instrument and the plasma to be quantified and modeled [1]. This model has been applied to the entire Van Allen Probes EMFISIS dataset in order to mitigate the impact of these effects on both the amplitude and phase of the measured electric field. A full sheath-corrected EMFISIS L4 dataset has recently been made available to the community.

The dynamics of Earth's outer electron radiation belt is, in part, driven by interactions with whistler-mode chorus waves. Chorus can cause rapid acceleration of electrons up to relativistic energies, as well as drive precipitation of particles into the atmosphere during microbursts and diffuse auroral precipitation. Chorus is typically observed between 0.05 and 0.90 f_{ce}, where f_{ce} is the equatorial electron cyclotron frequency. Prior to the development of the sheath corrected dataset, numerous studies directly investigated the electric field chorus wave power [2, 3], in part, because of how the high-amplitude parallel electric field component associated with oblique chorus [4] can drive nonlinear electron acceleration through Landau resonance [5]. The Poynting vector, which is determined from both magnetic and electric field observations, has also been investigated with results used to determine the chorus source region location, size, and dynamics [6, 7, 8]. Here, we perform direct comparisons between the uncorrected observations and the sheath-corrected chorus wave data, quantifying the impact of the sheath correction on the electric field wave power, as well as the Poynting vector magnitude and direction.

2 Chorus Identification

The first step in identifying chorus waves is to limit observations to time periods when the Van Allen Probes spacecraft are located outside of the plasmasphere. We further limit data based on wave measurements, isolating intervals with, i) waves above the instrument background levels observed between 0.05 and 0.90 f_{ce}, ii) ellipticity [9] and 2D degree of coherence in the polarization plane [10] greater than 0.5, and iv) planarity [11] greater than 0.6. These criteria ensure right-hand circularly polarized plane waves, as is expected for whistler-mode chorus.

The selection criteria for isolating chorus signals are based solely on magnetic field observations which are unaffected by sheath effects, meaning the same criteria are applicable to both the uncorrected and sheath-corrected data. Having extracted chorus waves from the extensive Van Allen Probes dataset, we statistically investigate wave characteristics, and perform a direct comparison between the uncorrected and sheath-corrected data.

3 Electric Field Wave Power

Figure 1 shows the median electric field power spectral density of chorus waves as a function of normalized wave frequency, f/f_{ce}, with the uncorrected data, E_w^{uncor}, and the sheath-corrected data, E_w^{cor}, shown in blue and red, respectively. It is evident that E_w^{cor} is significantly larger than E_w^{uncor} over the entire chorus wave frequency band. For lower frequencies, E_w^{cor} is a factor of ~2 larger than E_w^{uncor}. This factor increases with increasing wave frequency up to a local maximum of ~6 near 0.40 f_{ce}, decreases down to ~4 near 0.60 f_{ce}, before increasing again to a factor of ~9 by 0.90 f_{ce}. We do note that there are occurrences where these factors can substantially deviate from these median values, and whilst they may serve as a guide as to the impact of the sheath correction, the relative orientation between the spin-axis of the spacecraft and the background magnetic field has a strong impact on these quantities, since the sheath correction is applied in the instrument coordinate system.

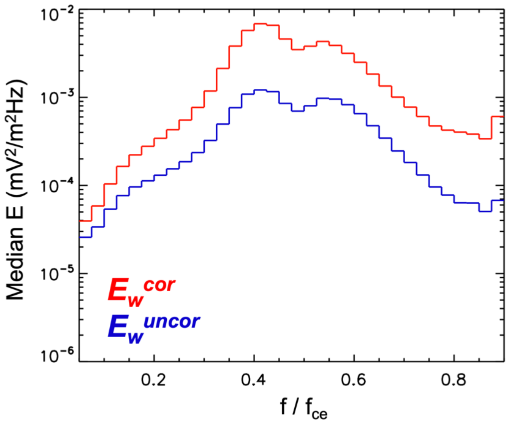

Figure 1. Median uncorrected, E_w^{uncor} (blue), and sheath-corrected, E_w^{cor} (red), electric field power spectra for chorus as a function of normalized wave frequency, f/f_{ce}.

Understanding how the sheath correction can impact the electric field chorus wave power is crucial given that the electric field can accelerate electrons through Landau and cyclotron resonances [12, 13, 14].

4 Poynting Vector

Since electric field observations are required to determine the Poynting vector, it too is impacted by the sheath correction. In a similar manner to the electric field analysis, the median spectrum of Poynting flux is determined using the uncorrected, S^{uncor}, and sheath-corrected, S^{cor}, data products. Figure 2 (top) shows S^{uncor} (blue) and S^{cor} (red) as a function of f/f_{ce}. It is evident that S^{cor} is larger than S^{uncor} for all frequencies. In comparison to the electric field observations where the factor between the uncorrected and sheath-corrected values showed a strong dependence on wave frequency, the factor between S^{uncor} and S^{cor} is relatively constant for all frequencies, with S^{cor} being a factor of ~2 greater than S^{uncor} over the entire chorus wave frequency band. Actual values vary between 1.30 and 2.55, depending on wave frequency.

The sheath correction not only affects the magnitude of the Poytning vector, but also its direction. The polar angle of the Poynting vector, θ_S, is defined as the angle between the Poynting vector and the background magnetic field. Numerous previous studies have used θ_S to determine the chorus source region location, size, and dynamics by investigating the position where θ_S transitions from propagation with a component parallel to the background magnetic field ($\theta_S < 90°$), to propagation with a component anti-parallel to the background magnetic field ($\theta_S > 90°$). Here, we quantify how the sheath correction may impact such studies by determining the percentage of observations where the sheath correction causes θ_S to flip hemispheres, from parallel to anti-parallel. The results of this analysis are presented in Figure 2 (bottom) as a function of f/f_{ce}.

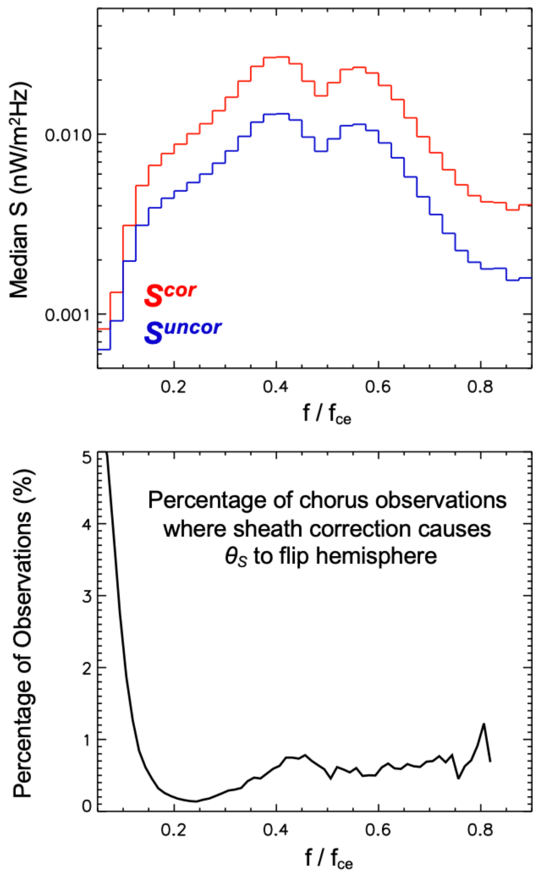

Figure 2. (top) Median Poynting flux spectra, S^{uncor} (blue), and S^{cor} (red), determined from the uncorrected and sheath-corrected electric field, respectively. (bottom) Percentage of observations where the sheath correction causes θ_S to flip hemisphere from $\theta_S < 90°$ to $\theta_S > 90°$, or vice-versa.

It is found that for low frequencies, up to 5.4% of observations flip hemisphere after the sheath correction has been applied. However, for f/f_{ce} values above 0.125 this percentage drops below 1%, and is typically only a few tenths of a percent. Considering all frequencies, we find that the Poynting vector determined from sheath-corrected observations is in the same hemisphere as the uncorrected value (parallel or anti-parallel to the background magnetic field) in ~98% of cases. As such, the sheath correction causes the Poynting vector to flip hemispheres in only ~2% of cases, with these primarily at low frequencies. We therefore conclude that previous studies which used Van Allen Probes observations of θ_S to determine the location, scale size, and dynamics of the chorus source region are likely to achieve the same result if repeated using the sheath-corrected data. Due to the different instrumentation and spacecraft orientation used during other missions, the impact of sheath effects may be different. As such, these results are only valid for the Van Allen Probes, with investigation of other missions (e.g., MMS) ongoing.

5 Comparison between *k* and *S*

For whistler-mode waves in a cold plasma, a theoretical relationship [15] exists between the wave vector, *k*, and the Poynting vector, *S*. Figure 3 shows the refractive index surface, *n*, in a cold plasma in the field-aligned coordinate system for a wave frequency of 1.5 kHz, an electron cyclotron frequency of 10 kHz, and a plasma frequency of 20 kHz. The Gendrin angle, θ_G, and the resonance cone, θ_R, are shown by dotted and dashed lines, respectively. For each wave vector, *k*, the Poynting vector, *S*, is normal to the refractive index surface. Let us consider two wave vectors defined by k_1 (red) and k_2 (blue). For k_1, the polar wave vector angle, θ_{k_1}, is less than θ_G, meaning that both k_1 and S_1 are oriented in the positive $n_\perp$ direction. For k_2, the polar wave vector angle, θ_{k_2}, is greater than θ_G, which results in k_2 being oriented in the positive $n_\perp$ direction, but S_2 being oriented in the negative $n_\perp$ direction.

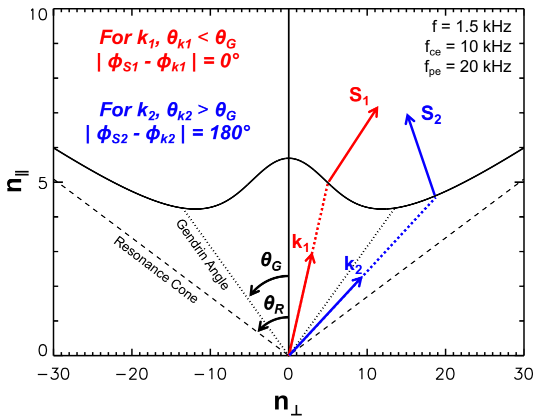

Figure 3. The theoretical relationship between the *k* and *S* for whistler-mode waves in a cold plasma.

As such, the absolute value of azimuthal angle of the wave vector subtracted from the azimuthal angle of the Poynting vector, $|\phi_S - \phi_k|$ is equal to 0° in the case of k_1 and S_1 but equal to 180° in the case of k_2 and S_2. This relation is true for all wave vector directions, meaning $|\phi_S - \phi_k|$ = 0° for $\theta_k < \theta_G$, and conversely $|\phi_S - \phi_k|$ = 0° for $\theta_k > \theta_G$. The validity of this relationship is explored using both the uncorrected and sheath-corrected data.

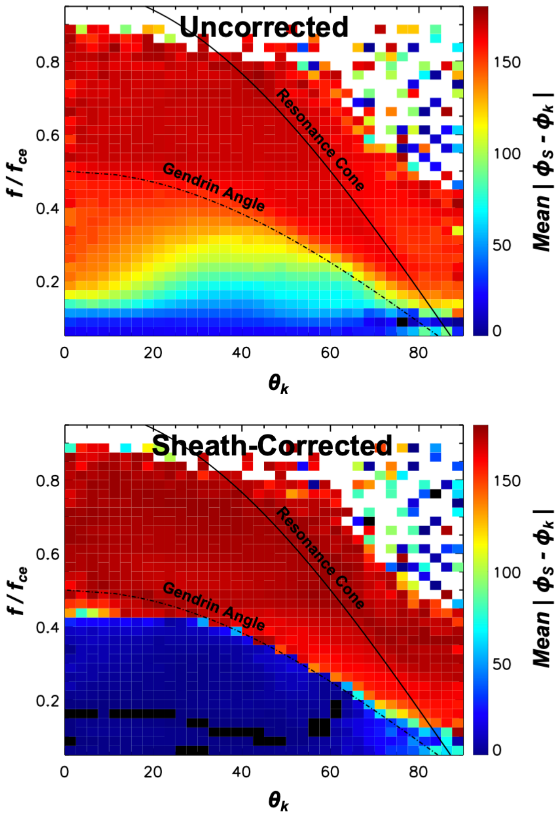

Figure 4. Mean $|\phi_S - \phi_k|$ as a function of f/f_{ce} and θ_k for (top) uncorrected and (bottom) sheath-corrected data.

Figure 4 presents the mean value $|\phi_S - \phi_k|$ as a function of wave normal angle, θ_k, and normalized wave frequency, f/f_{ce} for the (top) uncorrected observations and (bottom) the sheath-corrected data. The resonance cone, θ_R, and Gendrin angle, θ_G, are shown by solid and dot-dash lines, respectively. For lower band chorus ($f/f_{ce} < 0.50$), a strong frequency dependence is apparent in the relationship between *k* and *S* for the uncorrected observations. At frequencies near 0.05 f_{ce}, $|\phi_S - \phi_k|$ is near the expected value of 0°. However, as frequency increases, $|\phi_S - \phi_k|$ shifts away from 0° and by 0.20 f_{ce} is close to 90° even for θ_k values not near θ_G. For approximately field-aligned waves between 0.25 and 0.50 f_{ce} and $\theta_k < \theta_G$, $|\phi_S - \phi_k|$ is near 180°. In this region, there may be substantial scatter, as small fluctuations in the direction of *k* may result in large changes in ϕ_k. However, this relationship of $|\phi_S - \phi_k|$ being close to 180° remains apparent even for θ_k values greater than 30° above 0.30 f_{ce} and with $\theta_k < \theta_G$. This is in conflict with the expected relationship shown in Figure 3. For the sheath-corrected observations the relationship between *k* and *S* is much closer to that expected, being near 0° for $\theta_k < \theta_G$ and being near 180° for $\theta_k > \theta_G$, with the transition being well-defined by the $\theta_k = \theta_G$ boundary. Some deviation from this expected relationship is noted between 0.40 and 0.50 f_{ce} for $\theta_k < 30°$. This may be attributable to multiple factors, such as assuming a dipole field when determining the equatorial f_{ce} value, ϕ_k not being well-defined for small θ_k, the discrete frequency bins in the EMFISIS survey data blurring the f/f_{ce} = 0.50 boundary, or some other effect which is not yet known.

However, comparison between the uncorrected and sheath-corrected data presented in Figure 4 demonstrates that the expected relationship between *k* and *S*, as shown in Figure 3, is generally well reproduced by the sheath-corrected data, whereas significant deviations from the expected relationship exist in the uncorrected observations.

6 Conclusions

In this study, a direct statistical comparison of chorus wave properties derived from the uncorrected and sheath-corrected Van Allen Probes EMFISIS data has been performed. It is found that the sheath-corrected electric field chorus wave power is typically a factor between 2 and 9 times larger than the uncorrected observations, depending on wave frequency. The Poynting flux determined from the sheath-corrected data is typically a factor of ~2 larger than that obtained using the uncorrected observations. The sheath correction causes the polar angle of the Poynting vector, θ_S, to flip hemisphere in only ~2% of chorus wave observations. The uncorrected and sheath corrected datasets are tested against the theoretical relationship between the *k* and *S* for whistler-mode waves in a cold plasma. This relationship is well-reproduced by the sheath-corrected data, whereas the uncorrected observations show significant deviations from these expected values.

Overall, this study provides the first direct comparison between the sheath-corrected electric field observations and the uncorrected data product, quantifying the impact that the sheath correction has on chorus wave observations. These results help frame the context of previous studies based on uncorrected electric field wave observations by providing statistically averaged values describing the impact of the sheath correction on chorus wave properties.

Acknowledgements

NASA Grant 80NSSC21K0519. EU's Horizon 2020 grant agreement No. 870452. MSMT grant LUAUS23152.

References

[1] D. P. Hartley et al., “Quantifying the sheath impedance of the electric double probe instrument on the Van Allen Probes,” JGR: Space Physics, 127, e2022JA030369, 2022, doi:10.1029/2022JA030369.

[2] W. Li et al., “New chorus wave properties near the equator from Van Allen Probes wave observations,” Geophys. Res. Lett., 43, 4725-4735, 2016, doi:10.1002/2016GL068780.

[3] E. Tyler et al., “Statistical occurrence and distribution of high-amplitude whistler mode waves in the outer radiation belt,” Geophys. Res. Lett, 46, 2328-2336, 2019, doi:10.1029/2019GL082292.

[4] C. Cattell et al. “Discovery of very large amplitude whistler-mode waves in Earth's radiation belts,” Geophys. Res. Lett., 35, L01105, 2008, doi:10.1029/2007GL032009.

[5] A. V. Artemyev et al., “Non-diffusive resonant acceleration of electrons in the radiation belts,” Phys. Plasmas, 19(12), 122901, 2012, doi:10.1063/1.4769726.

[6] M. J. LeDocq, “Chorus source locations from VLF Poynting flux measurements with the Polar spacecraft,” Geophys. Res. Lett., 25(21), 4063-4066, 1998, doi:10.1029/1998GL900071.

[7] O. Santolik et al., “Central position of the source region of storm-time chorus”, Planet. Space Sci., 53(1–3), 299-305, 2005, doi:10.1016/j.pss.2004.09.056.

[8] S. Teng et al., “A statistical study of the spatial distribution and source-region size of chorus waves using Van Allen Probes data”, Ann. Geophys., 36, 867-878, 2018, doi:10.5194/angeo-36-867-2018.

[9] O. Santolik et al., “Magnetic component of narrowband ion cyclotron waves in the auroral zone”, J. Geophys. Res., 107(A12), 1444, 2002, doi:10.1029/2001JA000146.

[10] O. Santolik, and D. Gurnett, “Propagation of auroral hiss at high altitudes”, Geophys. Res. Lett., 29(10), 2002, doi:10.1029/2001GL013666.

[11] O. Santolik et al., “Singular value decomposition methods for wave propagation analysis”, Radio Sci., 38, 1010, 2003, doi:10.1029/2000RS002523, 1.

[12] O. V. Agapitov et al., “Nonlinear local parallel acceleration of electrons through Landau trapping by oblique whistler mode waves in the outer radiation belt,” Geophys. Res. Lett., 42, 10,140-10,149, 2015, doi:10.1002/2015GL066887.

[13] Y. Omura et al., “Cyclotron acceleration of relativistic electrons through Landau resonance with obliquely propagating whistler-mode chorus emissions,” JGR: Space Physics, 124, 2795-2810, 2019 doi.org/10.1029/2018JA026374

[14] A. V. Artemyev et al., “Nonlinear electron acceleration by oblique whistler waves: Landau resonance vs. cyclotron resonance”, Phys. Plasmas, 20(12), 122901, 2013, doi:10.1063/1.4836595.

[15] U. Taubenschuss et al., “Poynting vector and wave vector directions of equatorial chorus”, JGR: Space Physics, 121, 11, 912-11,928, 2016, doi:10.1002/2016JA023389.